



# The suitability mapping of an urban spatial structure for earthquake disaster response using a gradient rain optimization algorithm (GROA)

Reza Aghataher<sup>a</sup>, Hamidreza Rabieifar<sup>b,\*</sup>, Najmeh Neysani Samany<sup>c</sup>,  
Hani Rezayan<sup>d</sup>

<sup>a</sup> Islamic Azad University, Civil Engineering Faculty, South Tehran Branch, Tehran, Iran

<sup>b</sup> Islamic Azad University, Civil Engineering Faculty, South Tehran Branch, Tehran, Iran

<sup>c</sup> Department of GIS and RS, Faculty of Geography, University of Tehran, Iran

<sup>d</sup> Department of RS-GIS, Faculty of Geographic Sciences, Kharazmi University, Tehran, Iran

## ARTICLE INFO

### Keywords:

Spatial structure  
Quake response  
Suitability analysis  
Fuzzy analytical hierarchical process  
Rain optimization algorithm  
Gradient descent

## ABSTRACT

The urban spatial structure has a prominent role in the earthquake response process which should primarily be assessed in the areas that are most vulnerable to earthquake hazards. Search and rescue teams need to map and identify the appropriateness of urban infrastructures for disaster reaction after a quake to enable ease of movement and quick assistance to the casualties. The key objective of this study is to compute the appropriateness of a municipal spatial structure for crisis reaction after a destructive earthquake, with an emphasis on finding the most critical areas (those that are prone to emergency response disruption). The main contribution involves improving a geographic information system (GIS)-based earthquake-triggered hybrid framework for suitability analysis using a fuzzy analytical hierarchical process (FAHP) and gradient rain optimization algorithm (GROA). The modifying of a rain optimization algorithm (ROA) to a GROA based on gradient descent is carried out to avoid local optima, which results in optimizing the identification process of the key locations for emergency response. The planned approach has been executed in Tehran, the capital of Iran. The implementation consequences reveal the supreme crucial areas for emergency response in the study area with a demonstration of the efficiency of the GROA compared to the basic ROA. Both indicate that these sites are located in the west and southwest, while the junction degree and width of the roads are the most significant factors affecting a city's suitability for emergency response. In addition, the GROA is less sensitive to local optima and more economical than the ROA. Moreover, several rescue experts and urban planners expressed their high satisfaction (95 %) with the five-level suitability map for prioritizing the deployments of troops along with the critical area maps for preventing heavy casualties produced by the GROA.

\* Corresponding author.

E-mail addresses: [reza\\_aghataher@yahoo.com](mailto:reza_aghataher@yahoo.com) (R. Aghataher), [h\\_rabieifar@azad.ac.ir](mailto:h_rabieifar@azad.ac.ir) (H. Rabieifar), [nneysani@ut.ac.ir](mailto:nneysani@ut.ac.ir) (N.N. Samany), [Hani.Rezayan@khu.ac.ir](mailto:Hani.Rezayan@khu.ac.ir) (H. Rezayan).

<https://doi.org/10.1016/j.heliyon.2023.e20525>

Received 22 April 2023; Received in revised form 27 September 2023; Accepted 27 September 2023

Available online 6 October 2023

2405-8440/© 2023 Published by Elsevier Ltd.

This is an open access article under the CC BY-NC-ND license

(<http://creativecommons.org/licenses/by-nc-nd/4.0/>).

## 1. Introduction

Earthquakes represent one of the utmost hazardous catastrophes that can affect humankind, particularly in urban areas [1–9]. Topical earthquakes in Iran [10,11] have shown that it is crucial to plan novel policies for crisis reaction. There have been three main earthquakes in Iran, each claiming between 30,000 and 50,000 lives with magnitudes over 7RM (on the Richter scale) [12]. In terms of the different steps of catastrophe management, comprising preparedness, mitigation, reaction, and retrieval, the ‘emergency response’ to disasters is strongly related to the urban spatial structure [9,13]. Cities are complex systems in which a population can live and grow with a certain level of infrastructure, safety, and security, as well as physical settings and facilities [9,14]. The urban spatial structure has a central role in disaster response, especially in earthquake management [15], as it determines the appropriateness level of a city for crisis reaction after an earthquake. Any hurdle that limits this movement should be documented as soon as an earthquake occurs (in the preparedness phase) [15–19].

The key objective of this paper is to measure the suitability of the urban spatial structure for emergency response after a destructive earthquake (5.5–6 on the Richter scale) with an emphasis on finding the most critical areas (those that are prone to emergency response disruption). The related research for solving this problem is divided into two categories. The first type is dedicated to determining the influence of the metropolitan spatial structure on a city’s suitability for emergency response following an earthquake, in areas such as the comfort of movement for pursuit and liberate processes [20–28]. For example [20], checked the results of earthquakes on tall constructions over 15 years. They established the consequence of the rust development degree on the level of damage and casualties [21]. evaluated the outcome of metropolitan spatial signs using satellite images. Metropolitan construction arranging was undertaken by categorizing diverse procedures of structures (e.g., numerous kinds of expenditure, infrastructure, and manufacturing structures) and exposed spaces (e.g., forests, civic grounds, and country parks), including their corporeal organization, connectivity, and area of resistant surfaces. Similarly [22], performed continuous monitoring of the fitness prestige of urban constructions. They dedicated the features of bridges to a quantity of robustness in a metropolitan area [29]. examined the main sorts of urban construction and availability after a quake event while also analyzing the relationship amid the movement and spatial arrangement of a metropolis [30]. studied major ecological and social issues, counting the susceptibility of the buildings, the complication of the path network, the landscape sight, the attendance of people unacquainted with the municipal strategy, and the deficiency of material on appropriate migration wayfinding strategies utilizing spatial multi-criteria analysis. These factors are considered vital components in historical hubs where conditions are generally not suitable for the safe evacuation of the inhabitants.

[31] computed the possessions of earthquakes in urbanized zones from a grid viewpoint to progress catastrophe evacuation. They established that road width is one of the most significant morphological basics of an urban organization, given the need for ease of movement for search and rescue operations following an earthquake [32]. evaluated the character of the built-up form and morphology of important expenditures in terms of safety and tractability after an earthquake, focusing on road features [23]. studied the effect of construction height, the degraded loam state, and the absence of principles for building and frame superiority as the chief issues that can affect the disaster reply stage [9]. identified population, land use, and physical and critical infrastructure, in addition to roads and open spaces, as the main constituents of metropolitan construction for spatial planning against earthquakes [33]. used a weighted linear combination (WLC) method for earthquake preparedness and post-disaster reaction. They utilized various participants to classify high-risk sectors, arrange emergency response zones, or highlight susceptible populations [34]. evaluated the character of a variety of geospatial data forms and the utilization of geospatial skills in the phases of a quake and demonstrated their importance in the different earthquake stages.

The second category has concentrated on an approach involving a suitability assessment and mapping for disaster response. Several researchers applied a geographic information system (GIS)-based multi-criteria decision analysis (MCDA) [35–42]. Generally, they illustrated the levels of suitability for emergency response after an earthquake via a zoning map and did not concentrate on the optimized identification of particular locations (such as those prone to disaster response disruption). Artificial intelligence [43] and evolutionary algorithms have mainly been used for optimizing procedures [44–50].

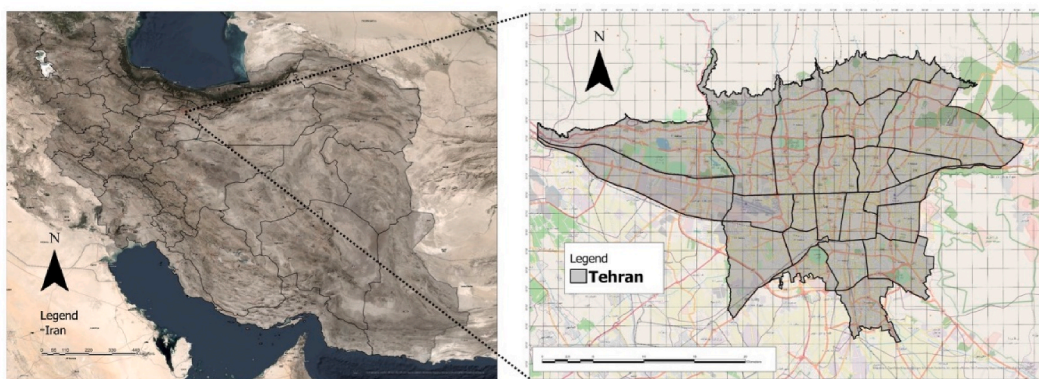


Fig. 1. Overview of the study area.

A review of the existing research shows that two important topics in this field need to be addressed: (1) not all essential risk issues relating to the urban structure that may affect rescue teams after an earthquake have been investigated, and (2) due to the diverse organization of large cities and different population densities, linear algorithms cannot identify the most critical points (those that are prone to emergency response disruption). In addition, conventional evolutionary algorithms may lead to local optima, decreasing the efficiency of the earthquake response. This paper attempts to evaluate the appropriateness of the urban spatial structure for disaster response after a destructive earthquake with an emphasis on highlighting the most urgent locations by improving a rain optimization algorithm (ROA) based on gradient descent.

## 2. Study area

The megalopolis of Tehran, the capital of Iran, consists of 22 districts and is located between latitudes 35°41'57" and 35°49'40" N and longitudes 51°19'55" and 51°30'57" E [6], as shown in Fig. 1. Tehran, which has an approximate population of 12 million and covers an area of 700 km<sup>2</sup>, is a hub of facilities, industries, and organizations. It is situated in the Middle East, in the southwestern part of Asia. Tehran is the greatest populated city in Iran and the Middle East (with approximately 10 million people). In geological terms, the faults in this city include the Mosha-Fasham, North Tehran, Niavaran, Telo Pa'in, Mahmoudieh, Shian, and South Rey ones. A possibility of fault activation has been identified in Mosha, South Rey, and North Tehran which could cause catastrophic damage.

## 3. Methodology

The purpose of this paper is to optimize the identification of critical emergency response sites (those that are prone to emergency response disruption) after an earthquake based on the urban spatial structure. Fault-binding sites are the most unsuitable locations, a conclusion reached through two key stages. The first step involved identifying the urban design criteria and sub-criteria associated with earthquake response, for which normalized maps were generated through spatial analysis. These were then weighted by a fuzzy analytical hierarchical process (FAHP) and overlaid using the weighted linear combination (WLC). The second step highlighted the critical sites for emergency response after an earthquake based on a ROA and a modified version, a gradient rain optimization algorithm (GROA). The earthquake scenario was considered severe [51], i.e., a magnitude 5.5–6 earthquake. Fig. 2 displays the stream diagram of the planned methodology.

### 3.1. Specification and structuring of criteria and sub-criteria

The spatial indices of the urban structure contribute significantly to the evacuation process as well as pursuit and release actions. Based on professional understanding and the works, the chief criteria in this regard are the roads, critical facilities, and land use, as well as the distance from natural features and the physical placement of buildings [9,52]. All the criteria and sub-criteria are depicted in Fig. 3 (the hierarchy is designed according to FAHP principles including criteria, sub-criteria, and a goal).

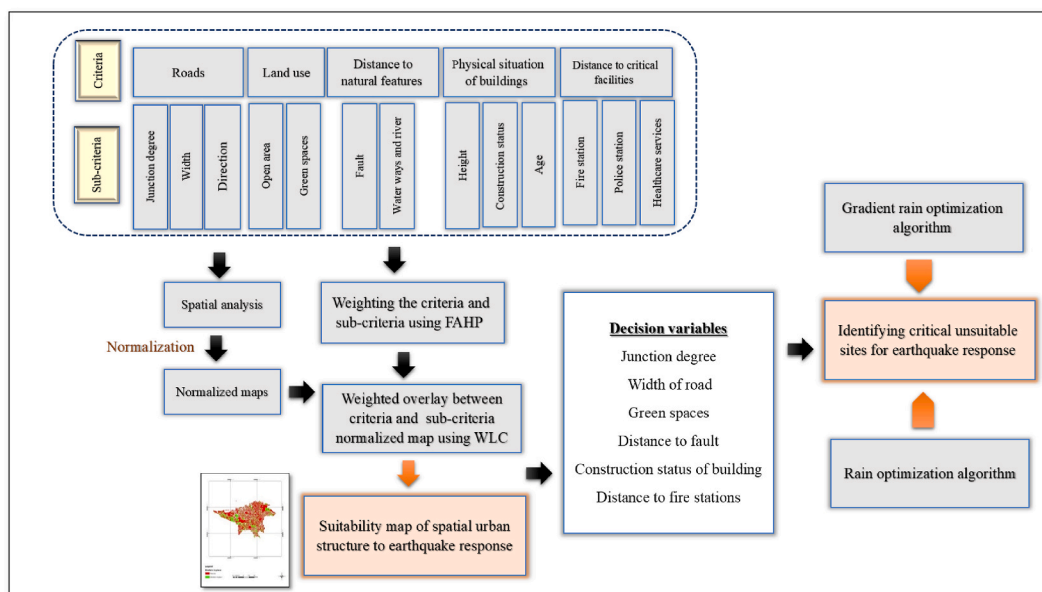


Fig. 2. A flow diagram of the planned method.

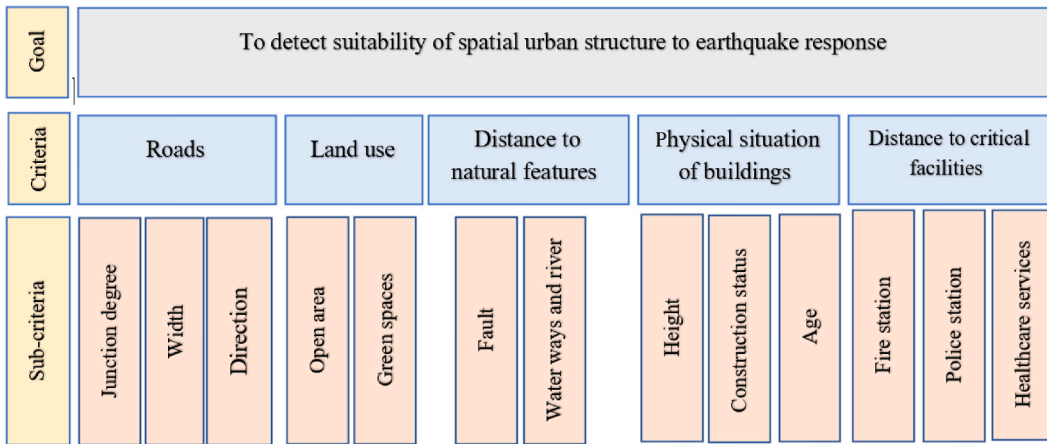


Fig. 3. The goal, criteria, and sub-criteria of an urban spatial structure.

3.1.1.1. Roads

Roads are among the essential sorts of metropolitan spatial configuration [53], and their various characteristics have a direct effect on a city’s suitability for crisis reaction after an earthquake, given the importance of ease of movement for search and rescue operations. A road has three main sub-criteria:

- **Junction degree:** The nodes in an urban traffic network are its connections. Nodes can include road junctures for drivers, sidewalks for pedestrians, and airports for business travelers. The foremost operative feature of a node is its connectivity score or grade based on the graph scheme (Fig. 4). This degree can be ranked by the value of the inward and outward ends. Weights can be specified on a gage from 5 (highways) to 1 (footpaths), consisting of public streets, overland streets, and urban roads [12].

Eq. (1) displays the formula for calculating the connection:

$$J_D = \sum_{i=1}^n W_i R_i \tag{1}$$

where  $W_i$  is the weight of the street (see Table 1) and  $R_i$  equals the number of roads associated with a node. The weights are demonstrated by specialists (13 metropolitan organizers and disaster managers).

- **Width:** street width is a factor that has a direct impact on the efficiency of disaster response (the wider the width, the easier way for movement) [54].
- **Road direction:** The street direction is essential for navigating the infrastructures. Typically, bi-directional ones are more possible than one-directional roads, as they allow for easier movement [55].

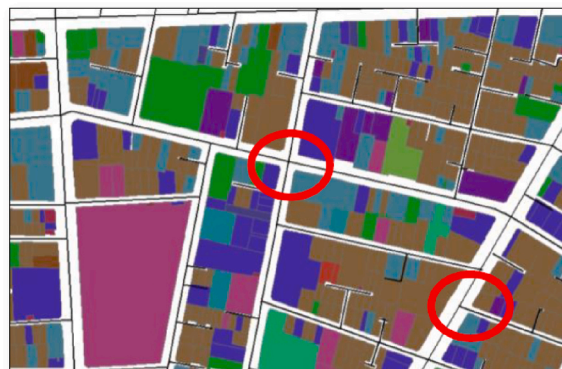


Fig. 4. An instance of the ‘connection degree’.

**Table 1**  
Streets weights (the description is defined based on [56]).

Street type	Weight	Description
Alley	0.2	A narrow lane, path, or walkway, habitually designed for walkers typically exists around buildings.
Avenue	0.4	A conventional route or path with a line of trees or large plants.
Boulevard	0.6	A broad, multi-lane roadway, habitually separated by a central median, that may have roadways and sideways on each side designed as slow travel and parking lanes, which may be employed for bike and pedestrian usage as well.
Main street	0.8	Wide streets with several lanes.
Highway	1	These types of roads are designed for high-capacity vehicular transport with structures such as several lanes. Vehicles usually travel at high speeds on these routes.

### 3.1.2. Land use

- **Green spaces:** Urban green spaces are any areas that are unoccupied and comprise wildlife and conservation parks. These sites are often more than 500 m<sup>2</sup> in area [8].
- **Open areas:** Open areas are usually spaces that are unconstructed and unrestricted, with an area generally greater than 500 m<sup>2</sup> [8].

### 3.1.3. Distance from natural features

In the study area, two main natural features may block the road or reduce the accessibility for search and rescue teams, namely faults and waterways.

- **Faults:** As most quakes are produced by dynamic faults, they are amongst the greatest critical issues and have a straight consequence on injury estimates. The superior the space from faults, the minor the probability of damage [51].
- **Waterways:** The distance from waterways is a vital issue that determines the possibility of waterlogging [11,37,57], as areas close to waterways are more likely to become waterlogged and less accessible following an earthquake.

### 3.1.4. Physical situation of buildings

- **Building age:** This indicates the quantity of time elapsed since a building’s structure. Higher age is associated with greater damage and road closures after an earthquake [7].
- **Building height:** High buildings by low suppleness will generally reduce a city’s appropriateness level for earthquake reaction [52], as they are more prone to damage. The height of buildings in the study area ranged between 4 and 90 m.
- **Construction status:** The quality of physical resources is one of the top criteria in deciding the susceptibility of metropolises to earthquake impairment. Based on the engineering system standards, the construction grade of a building is classified as unstable, worn-out, or stable [51], with unstable cities more prone to earthquake damage.

### 3.1.5. Distance from critical facilities

Critical facilities are the main amenities that could aid search and rescue teams during emergency response. The greater the accessibility to these facilities, the higher the city’s suitability for crisis reaction after an earthquake. Three sub-criteria were considered in terms of critical facilities, including fire stations, police stations, and healthcare centers [9].

## 3.2. Spatial normalization

The map quantities of all criteria were standardized based on Eqs. (2) and (3) [25]:

$$equalv_{maxij} = \frac{X_{ij} - X_{imin}}{X_{jmax} - X_{jmin}} \tag{2}$$

$$equalv_{minij} = \frac{X_{jmax} - X_{ij}}{X_{jmax} - X_{jmin}} \tag{3}$$

where  $v_{maxij}$  equals the normalized quantity of the maximized criterion,  $v_{minij}$  equals the standardized value of the minimized criterion,  $v_{minij}$  is equal to the normalized quantity of the minimized criterion,  $X_{ij}$  is the real quantity for the locality i and the pointer j,  $X_{imin}$  signifies the min quantity for the pointer j, and  $X_{jmax}$  is the max value for the pointer j.

## 3.3. FAHP-based criteria and sub-criteria weighting

The fuzzy analytical hierarchical process (FAHP) is a common MCDA approach applied for calculating qualitative values. The analytical hierarchical process (AHP) makes it possible to compare factors in pairs at different levels in a hierarchical structure. Moreover, fuzzy logic generally provides a simple method for making inferences regarding uncertainty and imprecise information

[25]. The step-by-step procedure for implementing an FAHP is demonstrated in Fig. 5. Based on the AHP design, a compound problem is classified into sub-problems in terms of ordered levels, with every hierarchy containing a group of criteria. The weights of these criteria were determined through pairwise grading as defined by Saaty [58]. The model’s robustness is measured using the consistency ratio (CR) via three elementary ethics, namely decomposition, relative ruling, and significance synthesis. The structures are rated as arithmetical quantities with the judgment matrix. Accordingly, the comparative weights of all features could be measured based on their hierarchical priority level. Table 2 shows the Saaty pairwise score rule. Numeric standards (1–9) are assigned according to the significance of the issues [59].

Considering the source of uncertainty in criteria weighting, a combination of fuzzy logic [61] with an AHP can present accurate results. Here, an object’s membership value signals its level of membership function [61]. This study used the triangular fuzzy number (TFN) and qualitative weights were considered for each category of fuzzy numbers (Table 3).

The following steps were taken to weigh the criteria using the FAHP:

• **Pairwise comparison**

All of the criteria in the graded system were applied to develop a pairwise comparison matrix. Pairwise evaluations were carried out using philological principles, with one of the two parameters being more relevant in all conditions. The AHP-based pairwise comparison was utilized for establishing judgment matrices (A), where  $A_n$  is the nth pointer component with  $A_{ij}$  as the decision matrix component (Eq. (4)).

$$A_{ij=(l,m,u)} = \left( \frac{A_{ij}}{A_{ji}}, u \right) \tag{4}$$

where l is the least possible quantity, m is the modest possible quantity, and u is the extremely probable quantity.

• **Calculating normalized weights**

The following equation was used to calculate the weights (fuzzy memberships).

$$W_n = GM / \sum_{n=1}^{N_j} GM_n \tag{5}$$

where GM is the arithmetical mediocre of the ith line of the verdict matrices and is obtained using Eq. (6):

$$GM = \sqrt[N_j]{A_{1n}A_{2n} \dots A_{nn}} \tag{6}$$

The feature vector method was employed to normalize the weights and eliminate the subjective ones. The CR of the topic variables and their groups was calculated to test the consistency of normalized values. A matrix’s CR shows its level of consistency against a

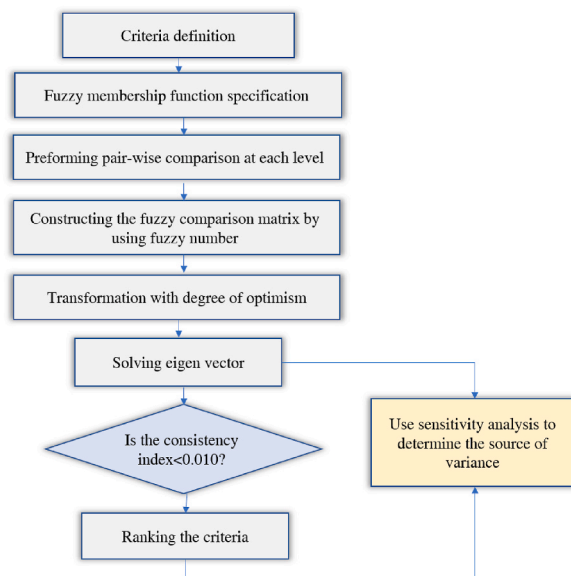


Fig. 5. FAHP stages.

**Table 2**  
The nine-point intensity of rank rule and its definitions [60]

Intensity of importance	Definition
1	Equal importance
2	Equal to moderate importance
3	Moderate importance
4	Moderate to strong importance
5	Strong importance
6	Strong to very strong importance
7	Very strong importance
8	Very to extremely strong importance
9	Extreme importance

**Table 3**  
Fuzzy number levels.

• Consistency assessment

Levels	Triangular fuzzy numbers	Reciprocal fuzzy numbers
Very low	(1,1,3)	(1,1,1/3)
Low	(3,4,5)	(1/3,1/4,1/5)
Medium	(4,5,6)	(1/4,1/5,1/6)
High	(5,6,7)	(1/5,1/6,1/7)
Very high	(7,7,9)	(1/7,1/7,1/9)

randomly created matrix [60].

The consistency index (CI) can be employed to calculate the accuracy of pairwise judgments as well as the consistency of judgments. This index controls the weight assignment balance. Although field experience is involved in weight allocation, over- and under-estimation are not allowed, and the figures must be as precise as possible. The satisfactory CR level is < 0.10 (Eq. (7))

$$CR = \frac{\text{Consistency Index}(CI)}{\text{Random Index}(RI)} \tag{7}$$

A matrix's CI is calculated by Eq. (8):

$$CI = \frac{\lambda_{max} - n}{n - 1} \tag{8}$$

where  $\lambda_{max}$  is the supreme quantity (weight) and n is the number of criteria. Coyle's chance key (RI) (Table 5) specifies the sum of the RI cost. Here, the higher value is on the order (value of n) of that of a random matrix and the lower row is the CI for arbitrary verdicts (Table 4).

3.4. Weighted overlay using a WLC

In this technique, the conclusion instruction computes the charge of each alternate through Eq. (9). Where  $V_{(a;k)}$  is the quantity of

**Table 4**  
Contradiction index of arbitrary quantities.

n	1	2	3	4	5	6	7	8	9	10	11	12	13	14	15
RI	0	0	0.58	0.9	1.12	1.24	1.32	1.41	1.45	1.49	1.51	1.48	1.56	1.57	1.59

**Table 5**  
The input spatial layers, output layers, and spatial analysis of the criteria.

Input layers	Spatial analysis	Output layers (sub-criteria map)
Road (Junction degree) - 1:2000 scale	Vector to raster (also Eq. 1)	Junction degree
Road (Width) - 1:2000 scale	Vector to raster	Width
Road (Direction) - 1:2000 scale	Vector to raster	Direction
Land use - 1:2000 scale	Vector to raster	Green space
Land use - 1:2000 scale	Vector to raster	Open area
Faults-1:2000 scale	Euclidean distance	Distance from faults
Waterways - 1:2000 scale	Euclidean distance	Distance from waterways
Parcels (Building age)	Vector to raster	Building age
Parcels (Building height)	Vector to raster	Building height
Parcels (Construction status)	Vector to raster	Construction status
Fire stations -1:2000 scale	Euclidean distance	Distance to fire stations
Police stations-1:2000 scale	Euclidean distance	Distance to police stations
Health-care centers	Euclidean distance	Distance to health-care centers

cell  $i$  based on criterion  $k$ ,  $W_k$  is the rank of criterion  $k$ , and  $V(a_{ik})$  is the ultimate quantity of yield cell  $i$ . [62]:

$$V(A_i) = \sum_{k=1}^n W_k V(a_{ik}) \tag{9}$$

### 3.5. Rain optimization algorithm (ROA)

The rain optimization algorithm is a type of evolutionary procedure developed based on the behavior of raindrops. The raindrops move to the lowest areas after reaching the ground (in this study, these represent the most unsuitable locations in terms of earthquake response, as they may be prone to disaster response disruption). Naturally, they can get stuck before reaching the marine level as the global minimum. The ROA simulates the inclination of droplets to move to the steepest slopes [63]. To clarify the ROA-based approach regarding the research problem, the process is explained in four steps, as illustrated in Fig. 6:

- A population of artificial raindrops is created randomly in the area of geographical terrain (the ‘very unsuitable’ and ‘unsuitable’ classes identified by the FAHP and WLC, called the rain optimization algorithm search space or ROASS in this research). The population number is denoted with  $n_{pop}$ . The position of each drop  $i$  is called  $X_i$ . Each drop could be active or inactive. Inactive drops are those that are either stuck, located far from the global optimum, or have stopped moving.
- The objective function is created based on the first six sub-criteria which have the highest scores based on expert ratings and the literature. The objective function value and its changes guide the iteration process.
- The natural movement behavior of artificial raindrops is simulated as they move to the steepest slope of the neighbor surrounding them. In this step, a neighborhood is generated for each drop and the algorithm assesses them through the objective function. The consequence of each neighboring point is compared with the prior location of the drop to specify which point resembles the deepest location of the zone. The neighborhood radius ( $R_a$ ) should be initialized ( $R_{in}$ ) at first, and each iteration can be different.
- This process is performed for each raindrop until the drop reaches the lowest point of the terrain (the most unsuitable area in the neighborhood in terms of earthquake response, as it may be prone to disaster response disruption) or gets stuck in a local optimum (one of the unsuitable areas in the neighborhood).

### 3.6. Modifying the ROA by gradient descent

The backpropagation (BP) algorithm is a strategy that assists in training artificial neural networks. The function of neural networks is based on repetition. There are two stages in each iteration. The first stage is when the artificial neural networks are formed and the values of the weights are randomly determined. The weights are assigned randomly because the exact values are not known. After determining the weights, the network then moves forward (feed-forward) by multiplying the input data by the weights and then summing it with the network bias. Finally, at the same stage, an output value is achieved that may differ from the actual output. After the network has identified the error according to the weights and biases, the network goes back and calculates the weights and biases again. This change means that the amount of error is reduced and the predicted value is closer to the actual value. When different values are expected from the neural network, the network considers this difference a fault. The procedure is fixed up to change the

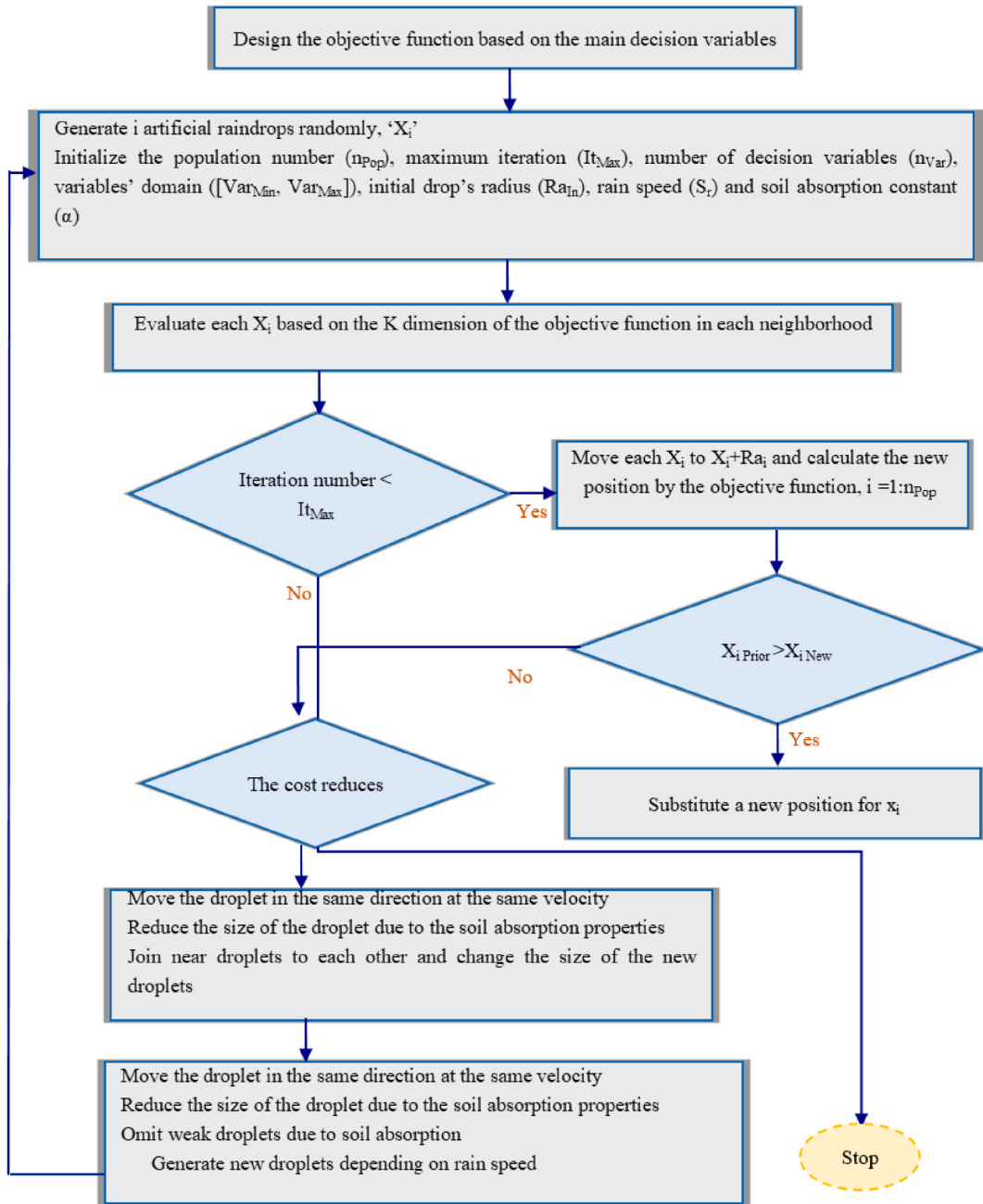


Fig. 6. Implementation of the rain optimization algorithm.

model parameters every time the output is unexpected. Therefore, once the parameter alters, the mistake similarly varied till the neural network discovers the anticipated production by calculating the gradient descent [64].

The BP strategy can be generalized to evolutionary algorithms such as the ROA. To modify the rain optimization algorithm, a new approach for tuning the rain speed ( $S_r$ ) parameters is considered, as stated in Eq. (10).

$$S_r(t+1) = \beta \Delta S_r(t) + \eta \delta_r(t) S_r(t) \tag{10}$$

where,  $S_r(t+1)$  is the speed of rain in time 't+1',  $\beta$  and  $\eta$  are the learning rate between [0,1], and  $\delta_r$  is the variance between the cost of the objective function in time 't' ( $E_t$ ) and 't-1' ( $E_{t-1}$ ) according to Eq. (11).

$$\delta_r(t) = E_t - E_{t-1} \tag{11}$$

### 4. Results

The implementation steps in the data preparation using spatial analysis and running the FAHP, WLC, ROA, and GROA are described as follows.

#### 4.1. Sub-criteria map generation through spatial analysis

The maps illustrating the urban design criteria related to earthquake response were generated using the data as well as spatial analysis (Table 5). These maps are presented in Fig. 7(a–j).

#### 4.2. Running the FAHP

The weighting process was performed using a questionnaire completed by 50 experts through questioning (24 specialists in disaster management, 14 in urban planning, and 12 in GIS). All the professionals determined the pairwise judgment and the last weights were planned utilizing Eqs. (4)–(8) in Expert Choice V11. The obtained criteria and sub-criteria weights with a satisfactory contradiction degree are presented in Table 6.

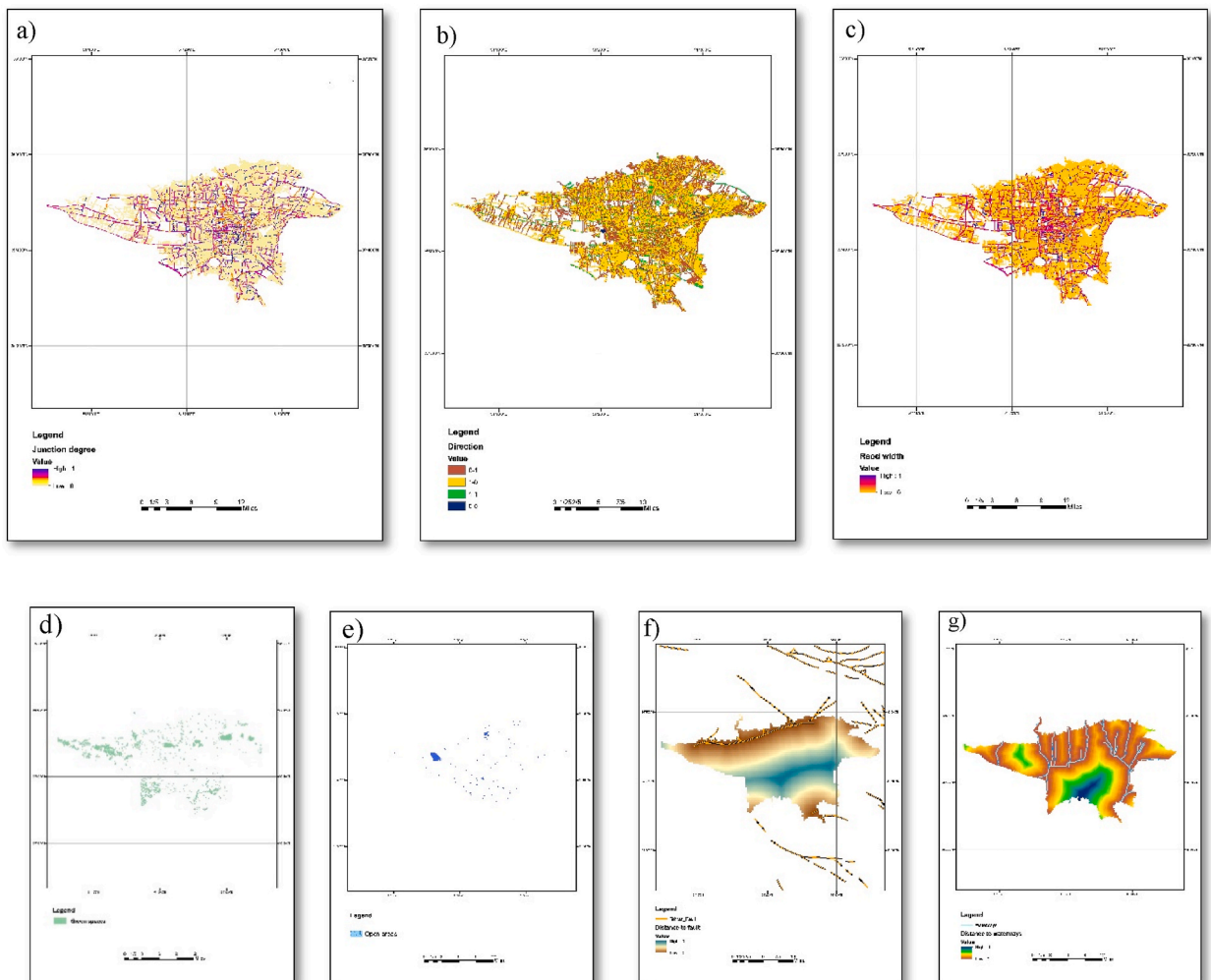


**Fig. 7.** Normalized sub-criteria maps: (a) connection degree, (b) direction, (c) road width, (d) green spaces, (e) open areas, (f) distance from faults, (g) space from waterways, (h) building height, (i) construction status, (j) building age, (k) space from fire stations, (m) space from healthcare cores, and (n) space from fire stations.

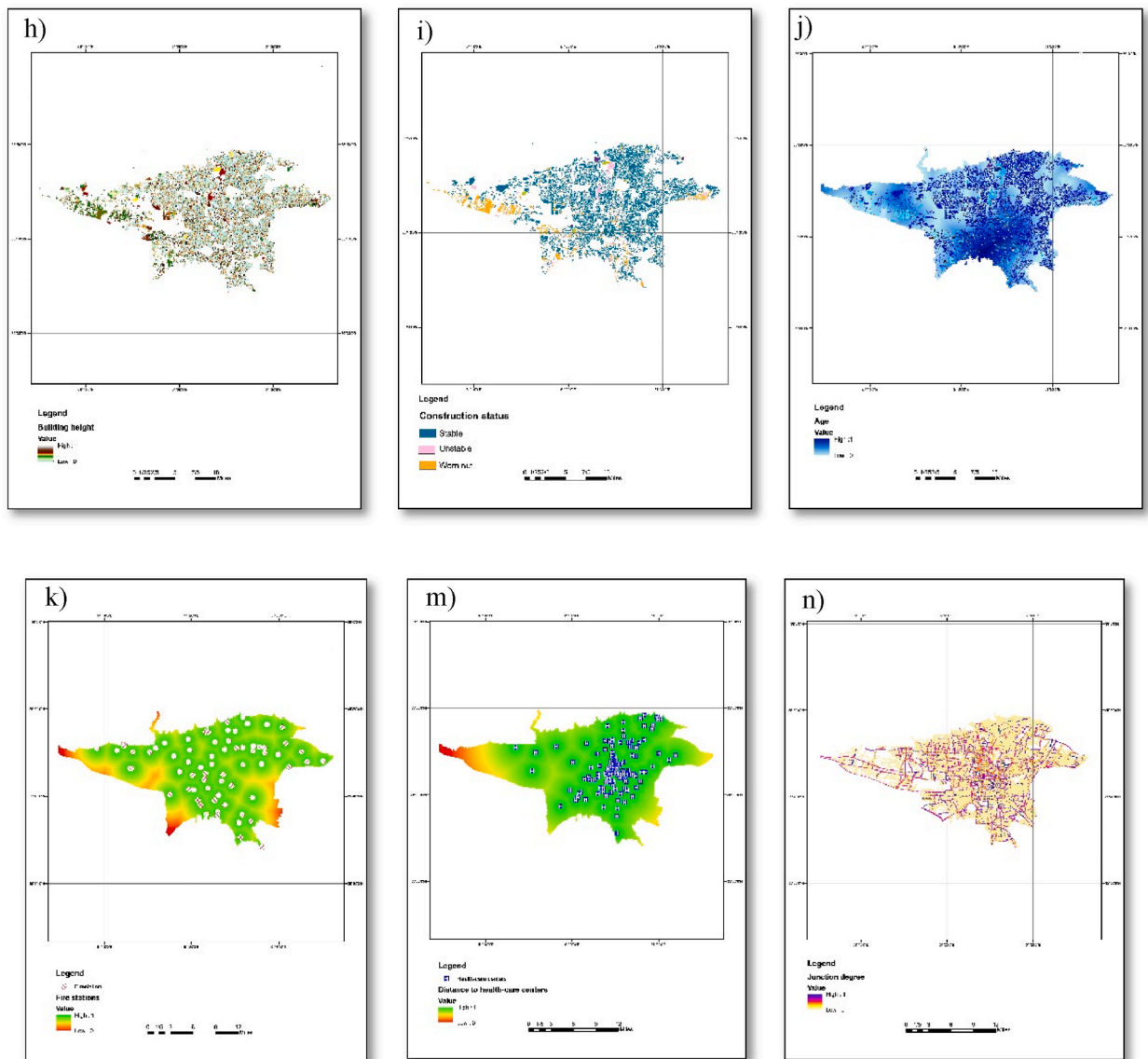


Fig. 7. (continued).

**Table 6**  
Weights of the criteria and sub-criteria achieved by the FAHP.

Criteria	Weight	CR	Sub-criteria	Weight	CR
Roads	0.31	0.061	Junction degree	0.48	0.045
			Width	0.38	
			Direction	0.14	
Land use	0.11		Green spaces	0.55	
			Open areas	0.45	
Distance from natural features	0.16		Faults	0.61	
The physical situation of the building	0.23		Waterways	0.39	
			Building age	0.21	
Distance from critical facilities	0.19		Construction status	0.45	
			Building height	0.34	
			Police stations	0.26	
			Fire stations	0.41	
			Healthcare centers	0.33	

### 4.3. Running the WLC

The WLC was utilized to combine the criteria and determine the suitability of the spatial municipal structure for disaster reaction after an earthquake through Eq. (9) and ArcGIS 10.3 via the ‘Raster calculator’ toolbox. A suitability map of the spatial urban construction was generated with five levels of suitability (classified by the natural break method), as shown in Fig. 8. Accordingly, 72 % of the study area has a ‘very suitable’ and ‘suitable’ status, while approximately 15 % is classified as ‘unsuitable’ and ‘very unsuitable’. The obtained map closely corresponds to the population density map (Fig. 9), indicating that approximately 1,200,000 persons are located in areas where providing an emergency response to a disaster is difficult.

### 4.4. Running the ROA and GROA

As shown in Fig. 6, the ROA and GROA have different parameters that should be adjusted based on the concern. These factors are the exploration universe, cost function, population number ( $n_{Pop}$ ), maximum iteration ( $It_{Max}$ ), number of decision variables ( $n_{Var}$ ), variables’ field ( $[Var_{Min}, Var_{Max}]$ ), original drop’s range ( $Ra_{In}$ ), rain speed ( $S_r$ ), and soil absorption constant ( $\alpha$ ) for both of the algorithms. For the GROA,  $\beta$ ,  $\eta$ , and  $\delta_r$  should be tuned.

In this study, the exploration universe consists of an appropriate class in the map resulting from the WLC (Fig. 8). Furthermore, six decision variables—including the junction degree, road width, construction status of the buildings, and green spaces, as well as the distance from faults and fire stations—were considered (they were selected based on the obtained suitability maps by experts). In addition, their quantities were planned consistent with the objective functions in Eqs. 12–18:

$$Obj_i = \left( \left( \frac{1}{N} \sum_{i=1}^N \sum_{j=1}^M JD_j D_{ij} * ij \right) / \overline{JDD} \right)^{-1} \tag{12}$$

where JD is the junction degree of the road and  $\overline{D}$  is calculated based on Eq. (11).

$$\overline{D} = \sqrt{\left( \frac{Xmax - Xmin}{2} \right)^2 + \left( \frac{Ymax - Ymin}{2} \right)^2} \tag{13}$$

**72%** of the region is in the ‘very suitable’ and ‘suitable’ classes  
**13%** is in the ‘moderate’ class  
**15%** is in the ‘very unsuitable’ and ‘unsuitable’ classes

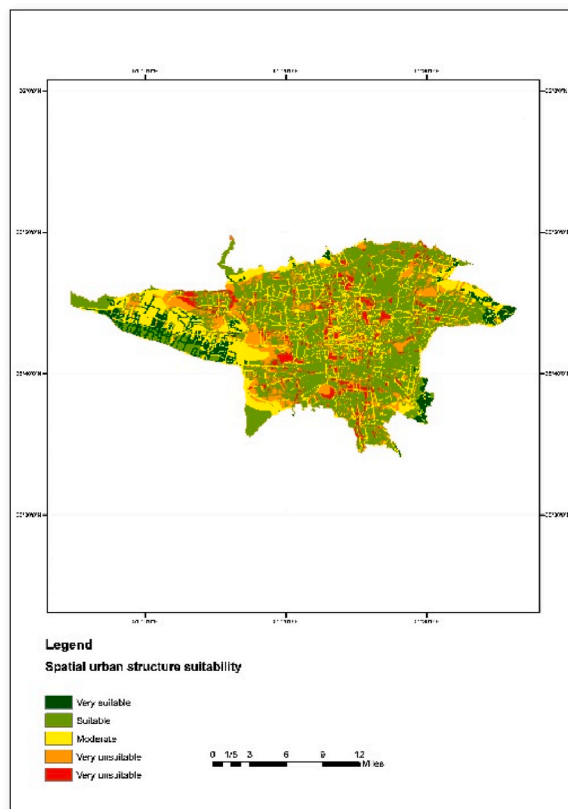


Fig. 8. Suitability map of the urban spatial structure.

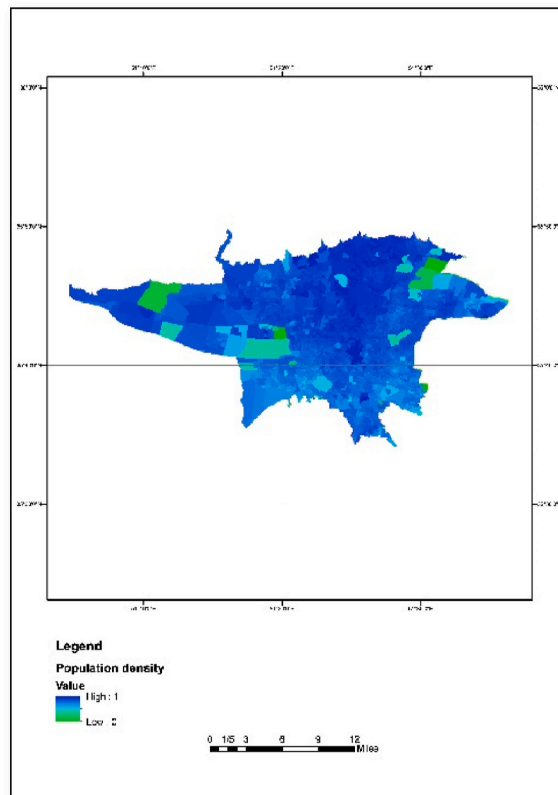


Fig. 9. Population density map of Tehran.

$$Obj_2 = \left( \left( \frac{1}{N} \sum_{i=1}^N Width_i \right) / \overline{Width} \right)^{-1} \tag{14}$$

$$Obj_3 = \left( \left( \frac{1}{N} \sum_{i=1}^N D.Geen\ space_i \right) / \overline{D. Greenspace} \right)^{-1} \tag{15}$$

$$Obj_4 = \left( \left( \frac{1}{N} \sum_{i=1}^N D.Fault_i \right) / \overline{D.Fault} \right) \tag{16}$$

$$Obj_5 = \left( \left( \frac{1}{N} \sum_{i=1}^N station \right) / \overline{D.Fire\ station} \right) \tag{17}$$

$$Obj_6 = \left( \left( \frac{1}{N} \sum_{i=1}^N \sum_{j=1}^M B_j D_{ij} * ij \right) / \overline{BD} \right) \tag{18}$$

**Table 7**  
Tuning parameters of the ROA.

ROA parameters	Experiment 1	Experiment 2	Experiment 3
The initial number of raindrops ( $n_{Pop}$ )	1000	1500	1200
Maximum iteration ( $It_{Max}$ )	100	150	200
Initial drop's radius ( $Ra_{In}$ )	15 m	10 m	10 m
Rain speed ( $S_r$ )	20 m/s	18 m/s	15 m/s
Cost function	0.0044	0.0031	0.0055

Number of decision variables ( $n_{Var}$ ): 6; Soil absorption constant ( $\alpha$ ): 0.2.  
Variables' domain ( $[Var_{Min}, Var_{Max}]$ ) is constant according to the database.

Where  $B$  is the construction status of buildings and  $\bar{D}$  is calculated based on Eq. (13). Consequently, the cost function is calculated as Eq. (19).

$$\text{Cost function} = w_{10}bj_1 + w_{20}bj_2 + w_{30}bj_3 + w_{40}bj_4 + w_{50}bj_5 + w_{60}bj_6 \quad (19)$$

Based on the selected decision variables and the defined cost function, 15 experiments were designed; the parameters for the top three are presented in Tables 7 and 8. According to the results of the ROA and GROA, Experiment 2 and Experiment 3 provided the best outcomes for each algorithm, and the following results were obtained based on their tuned parameters. Fig. 10 shows the convergence curves of the ROA and GROA based on Experiment 2 and Experiment 3, respectively. As can be seen, the GROA has converged significantly faster than the ROA, while it can also pass the local minima.

The ROA and GROA, as evolutionary algorithms, were able to identify the worst area of the urban spatial structure (the location most prone to emergency response disruption) in the specified neighborhood based on the defined decision variables. Fig. 11 shows the critical areas for emergency response after an earthquake, where access for recovery teams may be blocked, based on the results provided by the ROA and GROA, respectively. These conditions may hinder the ease of movement for rescue teams after an earthquake. Assessing the detected sites with Google Maps and matching the decision variables will help decision-makers enhance the urban structure for disaster preparedness.

The most critical areas (those that are prone to emergency response disruption) are located in the west and southwest of Tehran, while the other ones are distributed throughout the study area. An evaluation of these regions, as well as other distributed hotspots, indicates that the main factors are the junction degree and road width followed by the construction status of buildings.

As can be seen from the results, the GROA identified more critical areas than the ROA, especially in the western and southeast parts. Considering that the GROA detected these sites despite the high population density in these locations, the efficiency of using a modified version of the ROA is confirmed.

All the suitability and critical area maps obtained using the FAHP, ROA, and GROA were presented to rescue experts (28 individuals) and spatial urban planners (15 individuals). They were satisfied with the five-level suitability map for prioritizing the deployment of troops (87 %) along with the critical area map for preventing heavy casualties (91 % for the ROA and 94 % for the GROA). The GROA indicated the critical areas (those that are vulnerable to emergency response disruption) more accurately than the ROA.

## 5. Discussion

This paper focused on mapping urban suitability and identifying the critical areas prone to being blocked for emergency response by rescue teams after a severe earthquake. The initial property of the proposed scheme is connected to the practice of the FAHP, which can model the uncertainty in the ranking of criteria and sub-criteria by professionals. This investigation took into account all the relevant urban structural factors of a suitability assessment based on the literature as well as expert views [65]. The obtained five-level suitability map could help rescue planners and decision-makers prepare the appropriate equipment for opening blocked streets. The correlation of the resulting map with the population density confirms the importance of designing new strategies for urban planners to avoid heavy casualties in Tehran, the capital of Iran.

The second aim of the proposed method is to detect the critical sites of spatial urban structures (those prone to emergency response disruption) using the rain optimization algorithm. As a metaheuristic approach, it requires little or no expectations about the issue being improved and can explore great spaces of contender answers. The other significant feature of this research is the improvement of the ROA with the BP strategy (gradient descent), which attempts to minimize the objective function more quickly than the basic ROA, in addition to having the ability to pass the local optima. This property has been revealed in the final map of Fig. 11 (a).

Despite its clear advantages, the proposed procedure suffers from certain restrictions that should be investigated in upcoming studies. The proposed method was solitarily implemented in Tehran, so it cannot be generalized to other regions. For example, some cities have huge waterways and rivers or a specific spatial urban structure that will affect their suitability for emergency response following an earthquake. The method can be implemented in other places only by adopting the criteria, sub-criteria, and decision variables for optimization according to the city's characteristics. The model is independent of the data, as well as the complexity of the relationship between the input and output.

## 6. Conclusions

To assess the appropriateness of a spatial urban structure for crisis reaction after a destructive earthquake, this paper proposed a GIS-based earthquake-triggered hybrid framework using MCDA and evolutionary algorithms. In the first step, the main criteria consisting of roads, critical facilities, and the physical situation of buildings, as well as land use and distance from natural features, were defined and their sub-criteria were determined. The criteria and sub-criteria were ranked with the FAHP and overlaid with a weighted linear combination (WLC) to generate a suitability map of the urban structure. According to the results, 72 % of the study area has a 'very suitable' and 'suitable' status while approximately 15 % is classified as 'unsuitable' and 'very unsuitable'. The close correspondence of the obtained map to the population density map indicates that approximately 1,200,000 individuals are located in areas prone to disaster emergency response disruption.

In the second stage, six decision variables—including the junction degree, width of the road, distance from faults and fire stations, construction status of the building, and green spaces—were examined. These were selected according to assessments of the achieved

**Table 8**  
Tuning parameters of the GROA.

ROA parameters	Experiment 1	Experiment 2	Experiment 3
The initial number of raindrops ( $n_{Pop}$ )	1000	1500	1200
Maximum iteration ( $It_{Max}$ )	100	150	200
Initial drop's radius ( $Ra_{In}$ )	15 m	10 m	10 m
Rain speed ( $S_r$ )	Updated based on Eqs. (10) and (11)	Updated based on Eqs. (10) and (11)	Updated based on Eqs. (10) and (11)
Cost function	0.000081	0.000051	0.000021
$B, \eta$	0.2, 0.7	0.4, 0.5	0.6, 0.4

Number of decision variables ( $n_{Var}$ ): 6, Soil absorption constant ( $\alpha$ ): 0.2.

Variables' domain ( $[Var_{Min}, Var_{Max}]$ ) is constant according to the database.

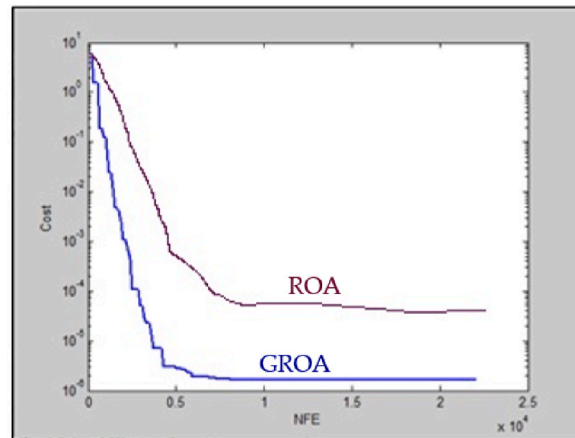


**Fig. 10.** The convergence curves of the ROA and GROA.

suitability maps by experts. The critical sites for emergency response after an earthquake (those that are vulnerable to emergency response disruption) have been identified based on the ROA and GROA. The implementation results of the proposed method had two main consequences from two viewpoints. First, the resulting maps from the ROA and GROA revealed that there are some areas prone to emergency response disruption following an earthquake, particularly in the west and southwest of Tehran, while some locations in the southeast parts have been added using the GROA. Assessing the detected sites with Google Maps and matching the decision variables will help decision-makers enhance the urban structure for disaster preparedness. The second achievement is related to the modification strategy of the ROA, which proved the efficiency of the GROA in decreasing the convergence time and accuracy of the results (by introducing some new critical sites).

The analysis of these regions, as well as other distributed hotspots, reveals that the most influential factors are the junction degree and road width, with the construction status at the next level of importance. In addition, the rescue experts expressed their satisfaction with the five-level suitability map for prioritizing the deployment of troops (87 %), along with the critical area map for preventing heavy casualties (91 % for the ROA and 94 % for the GROA).

According to the research findings, since some of these unsuitable areas are going to be populated shortly, there is a need for a vulnerability assessment in these regions. As a continuation of this work, the use of some other demographical factors to estimate the required resilience improvements for these locations is planned.

#### Data availability statement

Data will be made available on request.

#### Funding

The authors declare that no funds, grants, or other support were received during the preparation of this manuscript.

#### CRedit authorship contribution statement

**Reza Aghataher:** Conceptualization, Formal analysis, Methodology, Writing – original draft, Writing – review & editing. **Hami-dreza Rabieifar:** Data curation, Formal analysis, Software, Supervision, Validation, Visualization, Writing – review & editing. **Naj-meh Neysani Samany:** Data curation, Formal analysis, Methodology, Resources, Writing – review & editing. **Hani Rezayan:** Formal

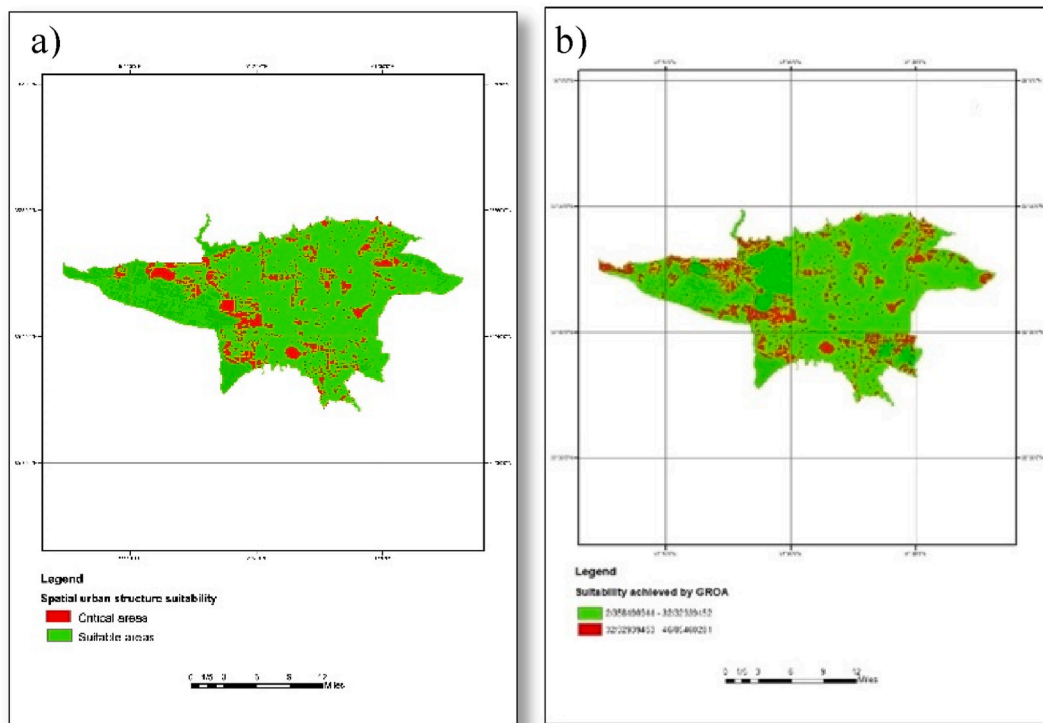


Fig. 11. The critical areas for emergency response after an earthquake are achieved by: (a) the ROA, and (b) the GROA.

analysis, Investigation, Resources, Writing – review & editing.

### Declaration of competing interest

The authors declare that they have no known competing financial interests or personal relationships that could have appeared to influence the work reported in this paper.

### References

- [1] F. Wang, Discussion on the methods analyzing urban earthquake vulnerability, *J. Seismol. Res.* 28 (2005) 95–101.
- [2] G.D. Bathrellos, H.D. Skilodimou, Land use planning for natural hazards, *Land* 8 (9) (2019) 128.
- [3] G.D. Bathrellos, H.D. Skilodimou, K. Chousianitis, A.M. Youssef, B. Pradhan, Suitability estimation for urban development using multi-hazard assessment map, *Sci. Total Environ.* 575 (2017) 119–134.
- [4] M. Karpouza, K. Chousianitis, G.D. Bathrellos, H.D. Skilodimou, G. Kaviris, A. Antonarakou, Hazard zonation mapping of earthquake-induced secondary effects using spatial multi-criteria analysis, *Nat. Hazards* 109 (1) (2021) 637–669.
- [5] S.K. Mohanty, R. Chatterjee, R. Shaw, Building resilience of critical infrastructure: a case of impacts of cyclones on the power sector in Odisha, *Climate* 6 (2020), <https://doi.org/10.3390/CL18060073>.
- [6] M. Rezaei, F. Amiraslani, N. Neysani Samani, S.K. Alavipanah, Application of two fuzzy models using knowledge-based and linear aggregation approach to identifying flooding prone areas in Tehran, *Nat. Hazards* 100 (2020) 363–385, <https://doi.org/10.1007/s11069-019-03816-9>.
- [7] Y. Asadi, N. Neysani Samany, K. Ezimand, Seismic vulnerability assessment of urban buildings and traffic networks using a fuzzy ordered weighted average, *J. Mt. Sci.* 16 (3) (2019) 677–688.
- [8] N. Neysani Samany, M. Sheybani, S. Zlatanova, Detection of safe areas in flood as emergency evacuation stations using modified particle swarm optimization with local search, *Appl. Soft Comput.* 111 (2021), 107681.
- [9] S. Kodag, Sh K. Mani, G. Balamurugan, S. Bera, Earthquake and flood resilience through spatial Planning in the complex urban system, *Progress in Disaster Science* 14 (2022), <https://doi.org/10.1016/j.pdisas.2022.100219>.
- [10] G.F. Karakaisis, Long-term earthquake prediction in Iran based on the time- and magnitude-predictable model, *Phys. Earth Planet. In.* 83 (2) (1994) 129–145.
- [11] M. Maybodan, M. Zare, H. Hamzehloo, A. Persan, A. Ansari, G.F. Panza, Analysis of precursory seismicity patterns in Zagros (Iran) by CN algorithm, *Turk. J. Earth Sci.* 23 (2014) 91–99, <https://doi.org/10.3906/yer-1212-6>.
- [12] M.R. Pourjafar, A.A. Taghvaei, Urban design criteria for earthquake preparedness in organic urban areas of Tehran, *J. of Hum* 12 (1) (2005) 13–20.
- [13] J. Liang, N. Xi, J. Liu, J. Yang, H. Shi, Z.h. Yang, Introduction to China's earthquake emergency response system, *Earth Sci.* 34 (5) (2021) 447–459.
- [14] D.R. Godschalk, Urban Hazard mitigation: creating resilient cities, *Nat. Hazards Rev.* 4 (3) (2003) 136–143, [https://doi.org/10.1061/\(asce\)1527-6988, 2003\) 4: 3\(136\)](https://doi.org/10.1061/(asce)1527-6988, 2003) 4: 3(136)).
- [15] E. Mavhura, T. Manyangadze, K. Raj, A composite inherent resilience index for Zimbabwe: an adaptation of the disaster resilience of place model, *Int. J. Disaster Risk Reduc.* 57 (2021), 102152, <https://doi.org/10.1016/j.ijdrr.2021.102152>.
- [16] J. Barrosa, H. Santa-Mariabc, Seismic design of low-rise buildings based on frequent earthquake response spectrum, *J. Build. Eng.* 21 (2019) 366–372.
- [17] E. Harirchian, T. Lahmer, Developing a hierarchical type-2 fuzzy logic model to improve rapid evaluation of earthquake hazard safety of existing buildings, *Structures* 28 (2020) 1384–1399.

- [18] I.E. Aigwia, O. Filippova, J. Ingham, R. Phipps, Unintended consequences of the earthquake-prone building legislation: an evaluation of two city center regeneration strategies in New Zealand provincial areas, *Int. J. Disaster Risk Reduc.* 49 (2020), 101644.
- [19] M.R. Alasiri, R. Chicchi, A.H. Varma, Post-earthquake fire behavior and performance-based fire design of steel moment frame building, *J. Constr. Steel Res.* 1771 (2021), 106442.
- [20] M. Çelebi, A. Sanli, M. Sinclair, S. Gallant, D. Radulescu, Real-time seismic monitoring needs of a building owner—and the solution: a cooperative effort, B.C., Canada August 1-6, in: Available from: 13th World Conference on Earthquake Engineering Vancouver, 2004, 3104.
- [21] E. Banzhaf, R. Höfer, Monitoring urban structure types as spatial indicators with CIR aerial photographs for a more effective urban environmental management, *IEEE Journal of Select Top in App Earth Observ and Rem Sens* 1 (2) (2008) 129–138.
- [22] P. Klikowicz, M. Salamak, G. Poprawa, Structural health monitoring of urban structures, *Procedia Eng.* 161 (2016) 958–962.
- [23] K.S. Pribadi, M. Abduh, R.D. Wirahadikusumah, N.R. Hanif, M. Irsyam, P. Kusumaningruma, E. Puri, Learning from Past Earthquake Disasters: the Need for Knowledge Management System to Enhance Infrastructure Resilience in Indonesia, *Int J of Dis Risk Reduct.*, 2021, 102424.
- [24] N. Neysani Samany, M.R. Delavar, N. Chrisman, M.R. Malek, FIA<sub>5</sub>: a customized Fuzzy Interval Algebra for modeling spatial relevancy in urban context-aware systems, *Eng. Appl. Artif. Intell.* 33 (2014) 116–126.
- [25] S. Nadizadeh Shorabeh, A. Varnaseri, M.K. Firozjaei, F. Nickraves, N. Neysani Samany, Spatial modeling of areas suitable for public libraries construction by integration of GIS and multi-attribute decision making: case study Tehran, Iran, *Lib & Inf Sci Res* 42 (2) (2020), 101017.
- [26] N. Neysani Samany, Automatic landmark extraction from geo-tagged social media photos using deep neural network, *Cities* 93 (2019) 1–12.
- [27] M. Jelokhani-Niaraki, N. Neysani Samany, M. Mohammadi, A. Toomanian, A hybrid ridesharing algorithm based on GIS and ant colony optimization through geospatial networks, *J. Ambient Intell. Hum. Comput.* 12 (2020) 2387–2407, <https://doi.org/10.1007/s12652-020-02364-6>.
- [28] A. Darvishi Boloorani, N. Neysani Samany, R. Papi, M. Soleimani, Dust source susceptibility mapping in Tigris and Euphrates basin using remotely sensed imagery, *Catena* 209 (1) (2022), 105795, <https://doi.org/10.1016/j.catena.2021.105795>.
- [29] G. D'Ovidio, D.D. Ludovico, G. Luigi La Rocca, Urban planning and mobility critical issues in post-earthquake configuration: L'Aquila City Case Study, *Procedia Eng.* 161 (2016) 1815–1819.
- [30] G. Bernardini, S. Santarelli, E. Quagliarini, M. D'Orazio, Dynamic guidance tool for a safer earthquake pedestrian evacuation in urban systems, *Comput, Environ and Urb Sys* 65 (2017) 150–165.
- [31] Q. Xia, Y. Wang, Addressing cascading effects of earthquakes in urban areas from a network perspective to improve disaster mitigation, *Int. J. Disaster Risk Reduc.* 35 (2019), 101065.
- [32] F. Giulian, A.D. Falco, V. Cutini, The role of urban configuration during disasters. A scenario-based methodology for the post-earthquake emergency management of Italian historic centers, *Saf. Sci.* 127 (2020), 104700.
- [33] B.B. Walker, N. Schuurman, D. Swanlund, et al., GIS-based multicriteria evaluation for earthquake response: a case study of expert opinion in Vancouver, Canada, *Nat. Hazards* 105 (2021) 2075–2091, <https://doi.org/10.1007/s11069-020-04390-1>.
- [34] M. Shafapourtehrany, M. Batur, F. Shabani, B. Pradhan, B. Kalantar, H. Özener, A comprehensive review of geospatial technology applications in earthquake preparedness, emergency management, and damage assessment, *Remote Sens* 15 (2023), <https://doi.org/10.3390/rs15071939>, 1939.
- [35] B. Feizizadeh, Th Blaschke, Land suitability analysis for Tabriz County, Iran: a multi-criteria evaluation approach using GIS, *J. Environ. Plann. Manag.* 56 (1) (2011) 1–23, <https://doi.org/10.1080/09640568.2011.646964>.
- [36] Y.G. Jia, H.X. Shan, C.W. Tang, W.J. Ma, GIS-based coastal area suitability assessment of geo-environmental factors in Laoshan district, *Nat. Hazards Earth Syst. Sci.* 12 (2012) 143–150.
- [37] S. Samanta, C. Koloa, D.K. Pal, B. Palsamant, Flood risk analysis in lower part of markham river based on multi-criteria decision approach (MCDA), *Hydrology* 3 (2016) 29, <https://doi.org/10.3390/hydrology3030029>.
- [38] A.P. Vavatsikos, O.E. Demesouka, K.P. Anagnostopoulos, GIS-based suitability analysis using fuzzy PROMETHEE, *J. Environ. Plann. Manag.* 63 (2020) 604–628, <https://doi.org/10.1080/09640568.2019.1599830>, 4.
- [39] T. Akamatsu, K. Yamamoto, Suitability analysis for the emergency shelter allocation after an earthquake in Japan, *Geosciences* 9 (8) (2019) 336, <https://doi.org/10.3390/geosciences9080336>.
- [40] S. Qureshi, S. Nadizadeh Shorabeh, N. Neysani Samany, F. Minaei, M. Homaei, F. Nickraves, J.J. Arsanjani, A new integrated approach for municipal landfill siting based on urban physical growth prediction: a case study mashhad metropolis in Iran, *Rem. Sens.* 13 (5) (2021) 949.
- [41] U. Iqbal, P. Perez, J. Barthelemy, A process-driven and need-oriented framework for review of technological contributions to disaster management, *Heliyon* 7 (11) (2021), e08405, <https://doi.org/10.1016/j.heliyon.2021.e08405>. ISSN 2405-8440.
- [42] C. Çetinkaya, E. Özceylan, M. Erbas, M. Kabak, Spatial suitability analysis for site selection of refugee camps using hybrid GIS and fuzzy AHP approach: the case of Kenya, *Int. J. Disaster Risk Reduc.* 77 (2022), 103062.
- [43] N. Nickdoost, H. Jalloul, J. Choi, An integrated framework for temporary disaster debris management sites selection and debris collection logistics planning using geographic information systems and agent-based modeling, *Int. J. Disaster Risk Reduc.* 80 (2022), 103215.
- [44] F. Hu, W. Xu, X. Li, A modified particle swarm optimization algorithm for optimal allocation of earthquake emergency shelters, *Int. J. Geogr. Inf. Sci.* 26 (9) (2012) 1–24.
- [45] B. Saediian, M.S. Mesgari, B. Pradhan, M. Ghodousi, Optimized location-allocation of earthquake relief centers using PSO and ACO, complemented by GIS, clustering, and TOPSIS, *ISPRS Int. J. Geo-Inf.* 7 (8) (2018) 292, <https://doi.org/10.3390/ijgi7080292>.
- [46] T. Mondal, N. Boral, I. Bhattacharya, J. Das, P. Pramanik, Distribution of deficient resources in disaster response situation using particle swarm optimization, *Int. J. Disaster Risk Reduc.* 41 (2019), 101308.
- [47] N. Soulakellis, Ch Vasilakos, S. Chatzistamatis, D. Kavrouidakis, G. Tataris, E.E. Papadopoulou, A. Papakonstantinou, O. Roussou, Post-earthquake Recovery Phase Monitoring and Mapping Based on UAS Data, *ISPRS International Journal of the geo-information*, 2020.
- [48] S. Moghtadernejad, B. Tyrone Adey, J. Hack, Prioritizing road network restorative interventions using a discrete particle swarm optimization, *J. Infrastruct. Syst.* 28 (4) (2022), 04022039.
- [49] G. Guido, S. Shaffiee Haghsheenas, S. Shaffiee Haghsheenas, A. Vitale, V. Astarita, Application of feature selection approach for prioritizing and evaluating the potential factors for safety management in transportation systems, *Computers* 11 (10) (2022) 145, <https://doi.org/10.3390/computers11100145>.
- [50] J. Kwon, Y. Zheng, M. Jun, Flexible spatio-temporal Hawkes process models for earthquake occurrences, *Spatial Statistics* 54 (2023), 100728, <https://doi.org/10.1016/j.jspasta.2023.100728>.
- [51] Y. Asadi, N. Neysani Samany, K. Ezimand, Seismic vulnerability assessment of urban buildings and traffic networks using fuzzy ordered weighted average, *J. Mt. Sci.* 16 (2019) 677–688, <https://doi.org/10.1007/s11629-017-4802-4>.
- [52] P. Jankowski, A.L. Zielinska, M. Swobodzinski, Choice Modeler: A Web-based Spatial Multiple Criteria Evaluation Tool, *Transaction in GIS* 12 (4) (2008) 541–561, <https://doi.org/10.1111/j.1467-9671.2008.01111.x>.
- [53] K. Lynch, *The Image of the City*, MIT Press.
- [54] S. Anbazhagan, A. Jothibasu, Geoinformatics in groundwater potential mapping and sustainable development: a case study from southern India, *Hydrol. Sci. J.* 61 (6) (2014) 1109–1123, <https://doi.org/10.1080/02626667.2014.990966>.
- [55] N.H. Razavi, S. Habibi, M. Tabibian, The role of urban structure in resiliency against earthquake, *Hoviatshahr* 12 (35) (2018) 29–38. <https://www.sid.ir/en/journal/ViewPaper.aspx?id=702127>.
- [56] <https://simplicable.com/news/streets>.
- [57] E.P. Glenn, K. Morino, P.L. Nagler, R.S. Murray, S. Pearlstein, K.R. Hultine, Roles of saltcedar (*Tamarix spp*) and capillary rise in salinizing a non-flooding terrace on a flow-regulated desert river, *J. Arid Environ.* 79 (2012) 56–65.
- [58] ThL. Saaty, How to make a decision: the analytic hierarchy process, *Eur. J. Oper. Res.* 48 (1) (1990) 9–26, [https://doi.org/10.1016/0377-2217\(90\)90057-1](https://doi.org/10.1016/0377-2217(90)90057-1).
- [59] G. Coyle, *The Analytic Hierarchy Process (AHP)*, Sociology, 2004.
- [60] T. Saaty, Decision making with the analytical hierarchy process, *Int. J. Serv. Sci.* 1 (1) (2008) 83–98.

- [61] L.A. Zadeh, Fuzzy sets, *Information and Control* 8 (3) (1965) 338–353, [https://doi.org/10.1016/S0019-9958\(65\)90241-X](https://doi.org/10.1016/S0019-9958(65)90241-X).
- [62] J. Malczewski, GIS-based land-use suitability analysis: a critical overview, *Prog. Plann.* 62 (1) (2004) 3–65, <https://doi.org/10.1016/j.progress.2003.09.002>.
- [63] A.R. Moazzeni, E. Khamchi, Rain optimization algorithm (ROA): a new metaheuristic method for drilling optimization solutions, *J. Petrol. Sci. Eng.* 195 (2020), 107512, <https://doi.org/10.1016/j.petrol.2020.107512>.
- [64] M. Alwakeel, Z. Shaaban, Face recognition based on Haar wavelet transform and principal component analysis via Levenberg-Marquardt backpropagation neural network, *Euro J Sci Res* 42 (2010) 25–31.
- [65] R. Aghather, N. Najmeh Neysani, H.R. Rabiei Far, H. Rezayan, The role of morphological spatial indices in the suitability of urban earthquake management, *Earth Observation and Geomatics Engineering* 6 (1) (2022).